

# Transcriptional and post-translational regulation of MITF mediated by bHLH domain during the melanogenesis and melanocyte proliferation in *Crassostrea gigas*

Yue Min<sup>a</sup>, Hong Yu<sup>a</sup>, Qi Li<sup>a,b,\*</sup>

<sup>a</sup> Key Laboratory of Mariculture (Ocean University of China), Ministry of Education, and College of Fisheries, Ocean University of China, Qingdao 266003, China

<sup>b</sup> Laboratory for Marine Fisheries Science and Food Production Processes, Qingdao National Laboratory for Marine Science and Technology, Qingdao 266237, China

## ARTICLE INFO

### Keywords:

E-box motif  
DNA-binding affinity  
Melanocyte development

## ABSTRACT

Melanocyte differentiation is orchestrated by the master regulator transcription factor MITF. However, its ability to discern distinct binding sites linked to effective gene regulation remains poorly understood. This study aims to assess how co-activator acetyltransferase interacts with MITF to modulate their related lysine action, thereby mediating downstream gene regulation, including DNA affinity, stability, transcriptional activity, particularly in the process of shell pigmentation. Here, we have demonstrated that the CgMITF protein can be acetylated, further enabling selective amplification of the melanocyte maturation program. Collaboration with transcriptional co-regulator p300 advances MITF dynamically interplay with downstream targeted gene promoters. We have established that MITF activation was partially dependent on the bHLH domain, which was well conserved across species. The bHLH domain contained conserved lysine residues, including K6 and K43, which interacted with the E-box motif of downstream targeted-genes. Mutations at K6 and K43 lead to a decrease in the binding affinity of the E-box motif. CgMITF protein bound to the E-box motif within the promoter regions of the tyrosinase-related genes, contributing to melanogenesis, and also interacted with the E-box motif within the TBX2 promoter regions, associated with melanocyte proliferation. We elucidated how the bHLH domain links the transcriptional regulation and acetylation modifications in the melanocyte development in *C. gigas*.

## 1. Introduction

The elucidation of gene expression networks, in conjunction with the upstream regulatory pathways dictating their manifestation, has been extensively investigated in the biology of melanocytes [1,2]. Pioneer of these cells are neural crest derived and guided by a diverse array of pathways, encompassing cyclic adenosine monophosphate (cAMP), Wnt, phosphatidylinositol 3-kinase (PI3K)/Akt, mitogen-activated protein kinase (MAPK), and among others [3]. Microphthalmia-associated transcription factor (MITF) has a prominent and central role at the core of these intricate signaling pathways governing melanocyte proliferation, differentiation, and survival [4]. Importantly, how does MITF achieve discriminative and dynamic activation of specific gene modules?

MITF, characterized by target elements of the basic-helix-loop-helix-leucine-zipper (bHLH-LZ), recognizes 6-bp E-box motifs flanked by 5' T residues or 3' A residues. Additionally, it can identify 11-bp M box with

the core motif CATGTG, allowing it to distinguish between specific target sites and MYC-MAX binding sites [5,6]. The recruitment of co-activators like p300/CBP further facilitates MITF's dynamic interaction with a subset of promoters [7]. However, these motifs failed to discriminate between targets associated with MITF's diverse biological functions, such as differentiation or proliferation [6]. A contributing factor may involve epigenetic modification. The examination of MITF target genes has revealed notably higher levels of H3K27 acetylation in gene bodies related to melanogenesis compared to those in cell cycle regulation [8]. Moreover, in response to an alkaline shift in melanosome homeostasis, the activation of p300/CBP led to an enhancement in H3K27 acetylation levels in the promoters of key melanogenesis-related genes like tyrosinase (TYR), tyrosinase-related protein (TYRP), and dopachrome tautomerase (DCT), ultimately catalyzing the process of melanogenesis [9]. H3K27 acetylation pattern is also observed in cell cycle genes, albeit to a lesser extent than in pigmented genes [10]. It is noteworthy that acetylation occurs not only in histones but also in

\* Corresponding author at: Key Laboratory of Mariculture, Ministry of Education, Ocean University of China, Qingdao 266003, China.  
E-mail address: [qili66@ouc.edu.cn](mailto:qili66@ouc.edu.cn) (Q. Li).

transcription factors, thereby affecting their function.

The T-box protein 2 (TBX2) is a member of the T-box gene family of transcription factors, contributing to the regulation of cell proliferation [11]. Its expression followed a cell-cycle-dependent pattern, with reduced levels observed during the G1 and early S phases, and increased expression during the late S and G2 phases [12]. Previous investigations have revealed that TBX2 is directly regulated by MITF [13], and serves as a direct transcriptional target of PAX3 in the melanocyte lineage [14]. The majority of studies on TBX2 have focused on melanomas, emphasizing its role in inhibiting senescence by downregulating p21<sup>CIP1</sup> expression [15]. TBX2 exerted a suppressive role by recruiting histone deacetylase activity (HDAC) and interacting with HDAC1, facilitating the targeting of HDAC1 to specific promoters [15]. Additionally, TBX2 exhibited expression in the melanocytes of the hair follicles, promoting melanocyte proliferation [16], while concurrently repressing the expression of TYRP1 [17]. This underscored its dual role in controlling melanocyte fates.

The Pacific oyster (*Crassostrea gigas*) is the most commonly farmed oyster worldwide and constitutes a major marine resource yielded through aquaculture. During the breeding of *C. gigas*, four distinct color morphs have been developed, including white, black, golden, and orange shell color [18–20]. The variety of shell color sparks curiosity, prompting multiple studies conducted to uncover the pigmentation mechanism. In this study, we demonstrated that *CgMITF* is critical for melanogenesis and melanocyte proliferation. We identified genes exhibiting a consistent pattern of regulation alongside pigmentation, and identified p300 to be a co-activator of MITF, altering histone acetylation levels. bHLH-LZ domain was important for MITF's biological functions, binding with E/M box motif to process melanogenesis or cell proliferation. Our findings not only confirmed the conservation of MITF gene function, but also provided insight into combing epigenetic analysis and transcriptional regulation to elucidate the detailed role of MITF function in pigmentation regulation.

## 2. Materials and methods

### 2.1. Animals and sampling

One-year-old strains Pacific oysters with black shells were sourced from Laizhou, Shandong, China. The oysters were acclimated in seawater for one week before the experiment. The left mantle edge was dissected and preserved differently based on its intended use. For TEM observation, the left mantle was fixed into 2.5 % glutaraldehyde. For immunofluorescence experiments, the mantle was fixed into 4 % paraformaldehyde (PFA) at 4 °C for 12 h, then dehydrated with methanol, and finally stored at –20 °C. For RNA detection, enzyme assays, ELISA analysis and protein quantification, the mantles were flash frozen using liquid nitrogen.

### 2.2. Transmission electron microscope observation

The mantles of black-shell-colored oysters were excised into 1mm<sup>3</sup> fragments and immersed in 2.5 % glutaraldehyde at 4 °C. Following fixation, the tissues underwent rinsing with 0.1 M phosphate-buffered saline (PBS) and a subsequent post-fixation in 1 % osmium tetroxide. Following this, the tissues were subjected to dehydration through a sequence of ethanol immersions before being embedded in resin. Finally, the ultra-thin sections (60 nm) were stained with heavy metal solutions and examined using a JEM-1200EX transmission electron microscope (JEOL, Japan).

### 2.3. Immunofluorescence assays

For the mantle tissues immunostaining of *C. gigas*, MITF, TYR, TYRP2, TBX2, OCA2, and acetylated pan antibody (PTMBio, PTM0101) were performed as primary antibodies. Paraffin-embedded sections

were prepared and treated with xylene and a gradient of ethanol (100 %, 95 %, 80 %, 70 %). Subsequently, the sections were treated with 0.01 M citrate buffer (pH 6.0) for antigen retrieval using microwave radiation for 30 min and then cooled naturally to room temperature. Following this, sections were blocked with 5 % bovine serum albumin (BSA) (Solarbio, China) for 1 h at room temperature, and subsequently incubated with primary antibodies diluted with PBS at 4 °C overnight. Except for acetylated pan antibody is commercially available, other antibodies are custom-made. After incubation, the sections were washed with PBST (1× PBS with 0.1 % Tween-20), and then were incubated with fluorescent secondary antibodies, including Alexa flour 488-conjugated Goat anti-mouse IgG (Sangon Biotech, China) and Cy3-conjugated Goat anti-Rabbit IgG (Sangon Biotech, Chins), diluted in PBS for 1 h at room temperature. The sections were then washed with PBS, counterstained with 4',6-diamidino-2-phenylindole (DAPI) (Beyotime, China), and mounted with an anti-fade medium. The fluorescence images were captured on confocal laser scanning microscope (Leica SP8, Germany).

### 2.4. RNA isolation, cDNA synthesis, and real-time PCR

Total RNA was extracted from mantle tissues using TRIZOL (Invitrogen, USA). The first strand of cDNA was synthesized in accordance with the manufacturer's protocol employing Evo M-MLV RT kit (AG, China). The specific primers used in this study were listed in the Table S1. The relative quantitative PCR was performed using SYBR Green Pro Taq HS (AG, China). The reaction volume was 20 μL, including 10 μL 2× SYBR Green Pro Taq HS Premix, 0.4 μL each of forward/reverse primers at a final concentration of 0.2 μM, 2 μL of cDNA template (diluted 10 times) and 7.2 μL of RNase-free water. The qPCR was performed using the LightCycler® 480 instrument (Roche, Switzerland). Elongation factor 1-α (ef1α) served as the internal reference genes for normalizing gene expression levels and relative gene expression levels were calculated using 2<sup>-ΔΔCT</sup> method.

### 2.5. In vivo MITF small molecule inhibitor treatment

The oysters were anesthetized using 1 M MgCl<sub>2</sub> to facilitate valve opening. The MITF small molecule inhibitor used was ML329 (MCE, USA), injected into the adductor at the concentration of 100 μg per individual. The control group of oysters was injected with Dimethyl sulfoxide (DMSO) (Sangon Biotech, China) as the vehicle. These injections were administered three times every two days. After the final injection, the oysters were sampled after 48 h.

### 2.6. In vitro mantle tissues cultivation treatment with protein and inhibitor

Prior to the experiment, the oysters were immersed in filtered seawater for 2 h, and subsequently cleaned with 75 % ethanol. The mantle tissues were then dissected into pieces, and subjected to six times washes with 1× PBS solution supplemented with Penicillin-Streptomycin-Gentamicin Solution (Beyotime, China), each lasting 10 min. Following this, the mantle tissues were washed with primary medium comprising Leibovitz's L-15 (Gibco, USA) and Medium 199 (Gibco, USA), supplemented with Penicillin-Streptomycin-Gentamicin Solution. The tissues were further sectioned into minced shape. They were then randomly divided into 24-well plates and cultured in a complete medium consisting of Leibovitz's L-15, Medium 19, FBS (Hyclone, USA), and Penicillin-Streptomycin-Gentamicin at 16 °C. The tissues were incubated with MITF of bHLH domain and TBX2 protein, with concentrations ranging from 0 μg to 50 μg. Additionally, the p300 small molecule inhibitor C646 (MCE, USA) was introduced to the medium at concentrations ranging from 0 μM to 40 μM. Following a 12 h incubation period, the samples were collected for further analysis.

## 2.7. Plasmid construction and luciferase reporter assay

The MITF and TBX2 promoter (2000 bp upstream of the transcription start site) were amplified using oyster genomic DNA and inserted upstream of luciferase cassette at the *SacI/HindIII* site of pGL3-basic (Progema, USA), employing primers specified in Table S1. The coding sequences of p300 and MITF were amplified from oyster cDNA and integrated into the *BamHI/EcoRI* site of pcDNA3.1(+) vector (Progema, USA). Truncated constructs of MITF, each containing specific domains, were generated from the MITF full-length recombinant pcDNA3.1 vector. Motif-directed mutagenesis for the TBX2 promoter was carried out using the Mut Express II Fast Mutagenesis Kit (Vazyme, China).

HEK293T cells were seeded in a 24-well plate (Corning, USA) and cultured in DMEM (Hyclone, USA) containing 1 % antibiotic and supplemented with 10 % FBS (Hyclone, USA), at 37 °C with 5 % CO<sub>2</sub>. Upon reaching 70 % confluency, the cells were ready for transfection. The cells were cultured with serum- and antibiotic- free medium when transfection. Lipofectamine 3000 (Invitrogen, USA) was used for transfection, employing a 1:1 ratio of promoter to transcription factor plasmids. The DNA-lipofectamine complexes were added to the medium drop by drop. Following a 48 h incubation period, the luciferase reporter analysis was conducted using the Dual-Luciferase Reporter Assay System (Progema, USA) according to the manufacturer's protocol. Firefly and Renilla luciferase activities were quantified using Synergy™ H1 (BioTek, USA).

## 2.8. Western blot

Total proteins were extracted from mantle tissues using lysis buffer (Beyotime, China) containing a protease inhibitor phenylmethanesulfonyl fluoride (PMSF). The protein concentration was determined following the protocols of the BCA protein kit (Beyotime, China). Subsequently, the proteins were denatured by boiling at 95 °C for 10 min in 5× loading buffer (Solarbio, China). A total of 20 µg protein from each sample was separated by 12.5 % SDS-PAGE (Sangon Biotech, China) and transferred onto polyvinylidene difluoride (PVDF) (Millipore, USA) membranes. These membranes were then blocked using 5 % non-fat dry milk (Sangon Biotech, China) and subsequently incubated with primary antibodies at 4 °C overnight. The primary antibodies included rabbit anti-TYR antibody (1:1000), rabbit anti-TYRP2 antibody (1:1000), rabbit anti-MITF antibody (1:5000), rabbit anti-CDK1 antibody (1:5000), rabbit anti-TBX2 antibody (1:2500), rabbit anti-OCA2 antibody (1:2700), and mouse anti-β-actin antibody (1:2500; Sangon Biotech, China). This was followed by incubation with a secondary HRP-labeled goat anti-rabbit IgG antibody (1:5000; Abclonal, China) or secondary HRP-labeled goat anti-mouse IgG antibody (1:1000; Beyotime, China) for 2 h at room temperature. Signals were detected using the SuperPico ECL Chemiluminescence Kit (Vazyme, China) with a GE ImageQuant LAS4000mini system (GE, USA).

## 2.9. Electrophoretic mobility shift assay

The recombinant CgMITF containing an N-terminal 6× His-tag was expressed using pET-32a and *Escherichia coli* BL21 (Sangon Biotech, China). The coding sequence of CgMITF (227–515 aa) and truncated CgMITF (402–460 aa) based on the domain prediction by NCBI. The recombinant plasmids were subjected to codon optimization by BGI genomics. They were then transformed into BL21, and a single colony was picked and grown in LB medium at 37 °C to an OD<sub>600</sub> of 0.6. Isopropyl β-D-1-thiogalactopyranoside (IPTG) was added to the medium for 4 h growth at 37 °C with a final concentration of 1 mM. The induced bacteria were centrifuged, collected, ultrasonicated, and purified using Ni-NTA agarose according to the manufacturer's instructions. Purified CgMITF proteins were concentrated using ultra-centrifugal filters (Millipore, USA). The protein concentration was determined following the protocols of the BCA protein kit (Beyotime, China). The biotin labeled primers were designed based on the binding sites and were listed in

Table S1. The primers were annealed at 95 °C for 5 min, and then cooled down to room temperature. EMSA experiments were performed using chemiluminescent EMSA Kit (Beyotime, China) in accordance with manufacturer's instructions. For each binding reaction containing 2 µl EMSA/gel shift binding buffer, 1 µl CgMITF protein (0.4 µg/µl), 1 µl of biotin labeled probes (0.2 µM). In the cold competition group, unlabeled probes (1 µl; 50 µM) were added. In the mutation group, mutated unlabeled probes (1 µl; 50 µM) were added. The mixture was then incubated at 25 °C for 30 min, and the DNA-protein complexes were separated by 6.5 % nondenaturing polyacrylamide gel at 120 V for 1 h in 0.5× TBE at 4 °C. After being transferred to the nylon membrane at 360 mA for 1 h, DNA-protein complexes were crosslinked using ultraviolet lamp. Subsequently, after blocking and washing, the signals were detected using the GE ImageQuant LAS4000mini system (GE, USA).

## 2.10. Chromatin immunoprecipitation

The chromatin immunoprecipitation assay was carried out using a BersinBio™ Chromatin Immunoprecipitation Kit in adherence to the manufacturer's instructions. The 0.2 g of mantle tissues were sectioned into 1mm<sup>3</sup> fragments and resuspended with 20 ml of 1× PBS solution containing 37 % formaldehyde, achieving a final concentration of 1 %. The mixture was rotated vertically at room temperature for 20 min to facilitate crosslinking. Following this, 2 ml of glycine was added for vertical mixing and neutralization at room temperature for 5 min. After centrifugation, the collected precipitation was washed with pre-cooled PBS twice, and then re-collected. The precipitation was then homogenized with a lysis buffer supplemented with protease inhibitor and DTT. Subsequently, the samples underwent ultrasonic lysis at 35 % power for a period of 15 min. Following centrifugation, the supernatant was incubated with agarose beads at 4 °C for 1 h. The supernatant was divided into three groups, with elution buffer designated for Input group, antibody for the IP group, and IgG for the IgG group, each being added accordingly. Both the IP group and IgG group were subjected to incubate at 4 °C overnight, while the Input group was preserved at −20 °C. Subsequently, both the IP group and IgG group were further incubated with protein A/G-beads for 30 min at room temperature. After binding, the supernatant was efficiently removed utilizing a magnetic grate, followed by two washes with wash buffer at room temperature. Upon elution of the beads, the supernatant was incubated at 65 °C for 6 h, followed by 37 °C for 2 h, and then 55 °C for 2 h. Finally, DNA extraction was performed using phenol/chloroform/isoamyl alcohol methods. The precipitated DNA was analyzed by PCR, with primer sequences detailed in Table S1.

## 2.11. Protein immunoprecipitation

The mantle tissues were treated with a lysis buffer containing a protease inhibitor (Beyotime, China). Subsequently, the supernatant obtained after centrifugation was utilized for further immunoprecipitation. Following this, the 3 µg targeted gene antibody was co-incubated with the magnetic-beads protein A + G (Beyotime, China) at 4 °C overnight. Then the 3 mg of protein samples were co-incubated with the antibody-protein A + G complex at 4 °C overnight. Finally, the targeted protein was eluted using 0.1 M Glycine-HCl, and neutralized with the 0.5 M Tris-HCl and 1.5 M NaCl.

## 2.12. Edu cell proliferation assay

HEK293T cells were seeded in confocal dishes (Corning, USA) and cultured in DMEM with 10 % FBS (Hyclone, USA) and 1 % antibiotic at 37 °C with 5 % CO<sub>2</sub>. Upon reaching 70 % confluency, 3 µg of truncated MITF recombinant plasmids were transfected and incubated for 36 h. Subsequently, 50 µM Edu (Ribobio, China) was added to the medium and incubated for 2 h. The medium was then removed, washed with PBS, fixed with 4 % PFA for 30 min, and incubated with 2 mg/ml glycine for

10 min. After washing with PBS, the cells were treated with 0.5 % Triton X-100 in PBS, followed by Apollo staining and DNA staining in the dark. The fluorescence images were obtained using confocal laser scanning microscope (Lecia SP8, Germany). The relative intensity of fluorescence was measured using Image J software [18].

### 2.13. Tyrosinase activity

The tyrosinase activity detection was conducted in accordance with the manufacturer's instructions (Solarbio, China). The 0.1 g of mantle tissues was homogenized with ice extract buffer. After centrifugation, the supernatant was collected and mixed with the reaction buffer. The absorbance was measured at 10 s and 50 min using a spectrophotometer at 475 nm after incubation at 25 °C.

### 2.14. Enzyme-linked immunosorbent assays

The content of melanin was detected using shellfish melanin ELISA kit (Ruixin, China) according to the manufacturer's instructions. The tissues were homogenized using PBS. After centrifugation, the supernatant was obtained and diluted with dilution buffer. The diluted samples were incubated with HRP-conjugate reagent, covered with an adhesive strip, and incubated for 60 min at 37 °C. Subsequently, each well was aspirated and washed, repeating the process for four times. The chromogen solution was added to each well, mixed gently and incubated for 15 min at 37 °C. Finally, the stop solution was added and the absorbance was determined using a spectrophotometer at 450 nm.

### 2.15. Statistical analysis

The data was analyzed with GraphPad Prism 7.0 and student's *t*-test was performed to obtain statistical significance. The  $P < 0.05$  was considered as statistically significant.

## 3. Results

### 3.1. Distribution of melanogenesis-related genes and acetylation modifications

To investigate the function of different folds of mantle tissues in the melanin formation process, we conducted observations of melanin staining and performed immunofluorescence analysis related to melanin-related genes. The melanin was primarily deposited in the inner fold and inner surface of the middle fold (Fig. S1). TYR, TYRP2, TBX2, OCA2 and MITF were predominantly located in three different folds, exhibiting slightly different distribution patterns (Fig. S2). TYR protein was mainly located in the inner surface of the inner fold, and the outer surface of the outer fold (Fig. S2-A). TYRP2 exhibited distribution across three folds, with notably stronger fluorescence observed in the inner fold and middle fold compared to the outer fold (Fig. S2—C). Furthermore, the colocalization of acetylation modification and MITF protein was overlapped in the inner fold and middle fold (Fig. 1-A). The acetylation pattern aligns consistently with the distribution of melanin deposition. Following this, the MITF protein was immunoprecipitated from black mantle tissues, and subsequently detected using an acetylated pan antibody, demonstrating that the MITF protein can be acetylated (Fig. 1-B).

### 3.2. Key lysine residues are required for stimulation of MITF transcriptional activation

We further analyzed the histone acetyl transferase activity of p300 with MITF. The results demonstrated multiple binding sites of p300 located upstream of 2Kb in the MITF promoter region (Fig. S3-A), and exhibited a dose dependent effect (Fig. S3—B). Further experiment was conducted to ascertain whether p300 could function as a co-activator,

facilitating the binding of the transcription factor MITF to TYR-related gene promoters. The dual luciferase reporter experiments clearly indicated that p300 evidently enhanced MITF's affinity for the TYR-related gene promoters (Fig. 1-C, D). In line with previous findings regarding p300's ability to acetylate MITF [6], the software prediction suggested that p300 can interact with MITF's bHLH domain and acetylate specific lysine residues, potentially K1, K5, and K6 (Fig. 1-E). These residues exhibited highly conserved across species within the MITF subfamily of bHLH-LZ transcription factors, including TFEB, TFE3, and TFEC (Fig. 1-E). Of the predicted acetylated residues, only K6 was conserved and located within the p300 protein interaction region (Fig. 1-F). Moreover, the structure of the E-box motif and the bHLH domain indicated that residues K6 and K43 within the bHLH domain interacted with the phosphate backbone within the basic region (Fig. 1-G).

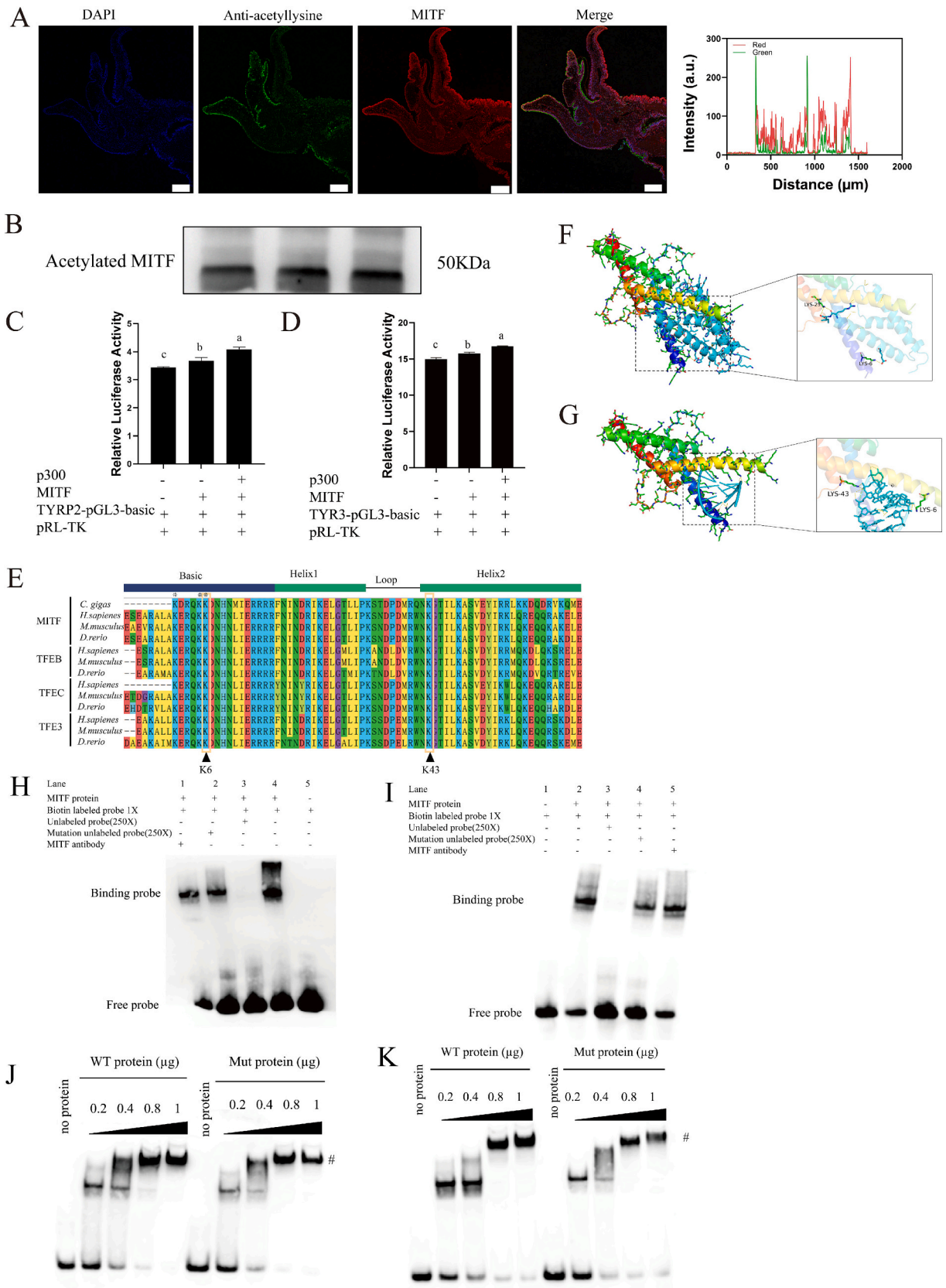
For our investigation into MITF binding affinity, we selected an enhancer associated with TYR-related genes. This particular enhancer was a well-established MITF target, and its binding has been demonstrated to be mediated by a 5'-CATGTG-3' motif, which was commonly found in validated MITF target genes [19]. Incubating the purified recombinant protein MITF (227–515 aa) with TYRP2 and TYR3 biotin probes resulted in a shift of the probe's mobility (Fig. 1-H; line 4; Fig. 1-I; line 2), indicating that this fragment of MITF was indeed capable of binding the enhancer. Both cold competitor probes exhibited no band (Fig. 1-H; line 3; Fig. 1-I; line 3), while the mutation probes displayed a relatively lighter band (Fig. 1-H; line 2; Fig. 1-I; line 4). This suggested that the mutation of the enhancer motif alone was insufficient to abolish binding, likely due to cooperative effects of the dimer. When no protein was added (Fig. 1-H, line 5; Fig. 1-I, line 1), the probe migration was not impeded. Next, we purified both the wild and mutant bHLH (K6R and K43R) domain of the MITF (402–470 aa), and incubated them with biotin probes respectively. The experiment revealed that the lysine mutant of bHLH domain displayed lighter binding band compared to the wild-type protein (Fig. 1-J, 1-K), indicating that key lysine residues can impact MITF-DNA binding. Taken together, these observations strongly suggested that the crucial lysine residues K6 and K43 could potentially play a pivotal role in modulating MITF function.

### 3.3. Inhibition of p300 correlates with reduced MITF transcriptional activity

In order to investigate the functional role of p300 in *C. gigas*, we performed in vitro cultivation of black mantle tissues following p300 inhibition with C646, a small-molecule inhibitor. As expected, MITF expression was significantly inhibited at both RNA and protein levels (Fig. 2-A, D, E). Additionally, the expression of MITF-targeted genes involved in melanogenesis (TYR, TYRP2, OCA2) was markedly reduced. We further analyzed genes related to melanocyte proliferation genes, such as TBX2, and CDK1, both of which exhibited significant suppression (Fig. 2-D, E). Furthermore, we immunoprecipitated the MITF protein from treated mantle tissues, allowing us to assess its interaction with binding proteins. Notably, the protein bands (TYR, TBX2, OCA2) were lighter than those in the control group (Fig. 2-F). Additionally, we detected tyrosinase activity and the melanin content after treatment, both of which showed significant reduction (Fig. 2-B, C). These results suggested that inhibition of p300, leading to the downregulation of MITF, potentially blocks the expression of its downstream effector genes.

### 3.4. MITF up-regulated exogenous expression promotes cell proliferation

Since we have identified the significance of p300-MITF signaling axis in melanogenesis, we hypothesized that CgMITF protein regulated melanocyte proliferation. To test this hypothesis, we overexpressed CgMITF in 293 T cells using different domains of CgMITF (Fig. 3-A). In contrast to the TFEB domain of CgMITF, the numbers of Edu-labeled cells increased in both the full length of MITF group and the bHLH domain of CgMITF group (Fig. 3-B, C). To further validate the role of



(caption on next page)

**Fig. 1.** p300 transcriptionally regulates MITF expression at proximal upstream regulatory regions of the MITF gene. (A) The co-expression of MITF and acetyllysine modification pattern in the mantle tissues was detected by immunofluorescence assay (Scale bars = 250  $\mu$ m). The colocalization was visualized using fluorescence intensity profiles across the arrow for both green and red channels, and was analyzed using Image J software. (B) Western blot using acetylated pan antibody of immunoprecipitated MITF. (C)(D) p300 function as the co-activator to enhance MITF binding to TYR promoters, as demonstrated by dual luciferase activity assays. (E) Alignment of amino acids in the basic region of related bHLH-LZ family members. The black triangle highlights highly conserved lysine residues. The asterisks represent the potentially acetylated sites. (F) The bHLH domain of MITF binds with p300 protein structure, wherein the K6 and K25 residues of bHLH interact with p300 protein. (G) The bHLH domain of MITF binds with E-box motif, wherein the K6 and K43 residues of bHLH interact with E-box motif. (H)(I) The EMSA was performed to validate the binding of MITF protein to the E-box motif in the TYRP2 and TYR3 promoter region. (J)(K) The wild-type bHLH domain protein and the mutated bHLH domain (K6R, K43R) protein were employed to assess their binding affinity to the E-box motif in the TYRP2 and TYR3 promoter region. The symbol “#” denotes the binding band. WT protein represents the wild-type bHLH domain of MITF, while Mut protein signifies the bHLH domain where lysine (K) 6 and lysine (K) 43 have been mutated into arginine (R).

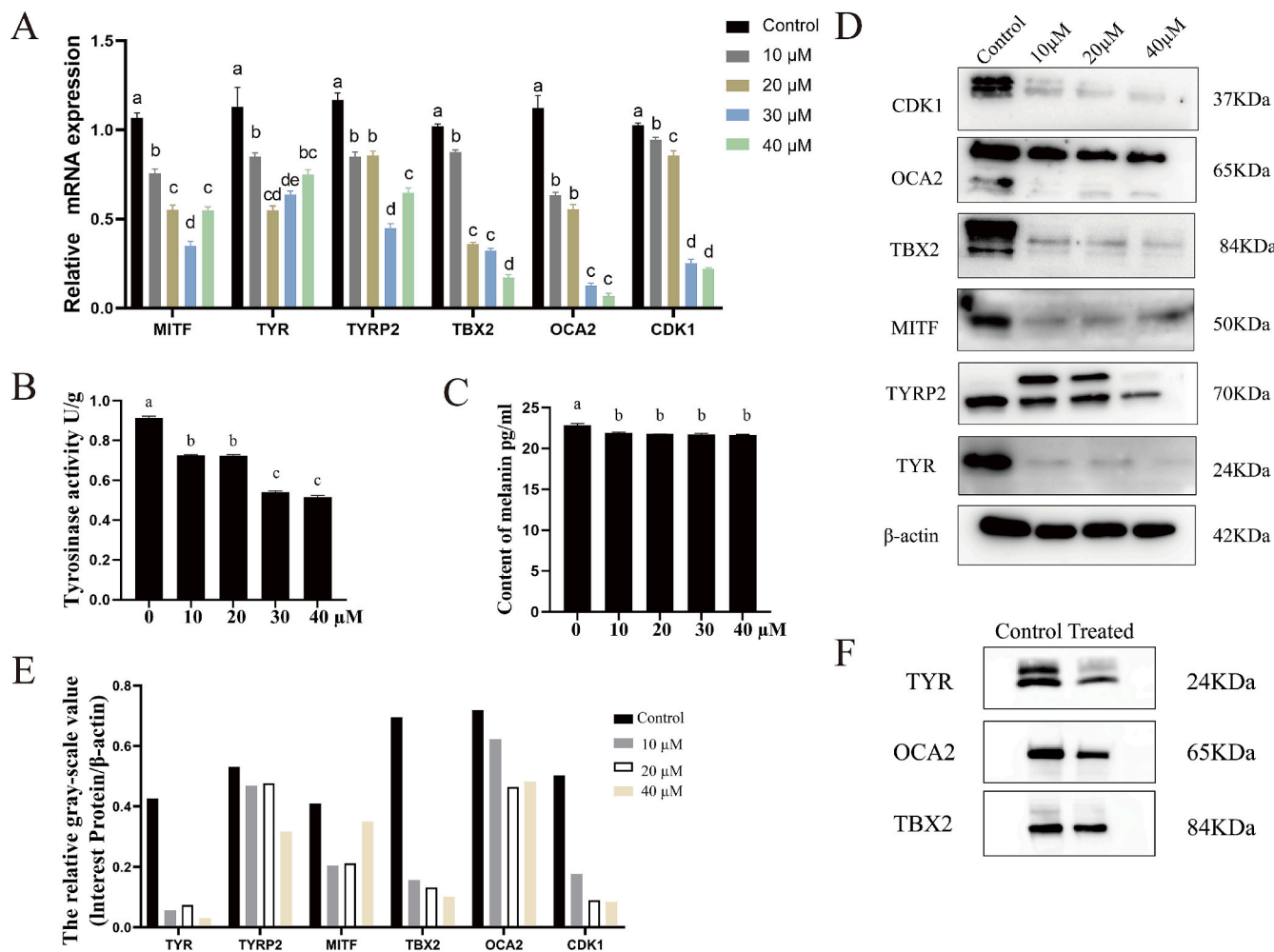


**Fig. 2.** Chemical inhibition of p300 HAT activity suppresses the p300/MITF/TBX2 transcriptional axis in vitro. (A) Gene expression analysis using qRT-PCR of MITF, TYR, TYRP2, OCA2, TBX2, and CDK1 upon p300 inhibition using C646 at different concentration. (B)(C) The tyrosinase activity and the content of melanin were detected after p300 was inhibited. (D) The protein expression level of TYR, TYRP2, OCA2, TBX2, CDK1, and MITF were detected and normalized with  $\beta$ -actin. (E) Protein band density was calculated using Image J software. (F) The MITF protein was immunoprecipitated from both control group and the C646 treated group. The interacting protein was subsequently detected using western blot analysis on the IP-MITF protein samples.

CgMITF in melanocyte proliferation and melanogenesis, we obtained recombinant CgMITF-bHLH protein and incubated it with black mantle tissues in vitro. Our statistical analysis revealed an upregulation in the mRNA expression of melanogenesis-related genes (TYR, TYRP2, OCA2) and melanocyte proliferation genes (TBX2, and CDK1) with different doses of protein incubation, particular at 10  $\mu$ g and 15  $\mu$ g (Fig. 3-D). The protein levels were detected under incubation with 10  $\mu$ g and 15  $\mu$ g, with the results consistent with the RNA expression level.

### 3.5. Targeting MITF with small molecule inhibitor: impact on melanin synthesis and melanocyte proliferation

To further validate that the bHLH domain of CgMITF mediates melanogenesis and melanocyte proliferation through MITF downstream targeted genes, we administered the ML329 small-molecule inhibitor in vivo three times every 2 days. Molecular docking revealed that ML329 could target with the bHLH domain of CgMITF (Fig. 4-A). Both the mRNA and protein expression analysis demonstrated a significant inhibition of melanogenesis-related genes and melanocyte proliferation genes compared to the control group (Fig. 4-B, E, F). Subsequently, we

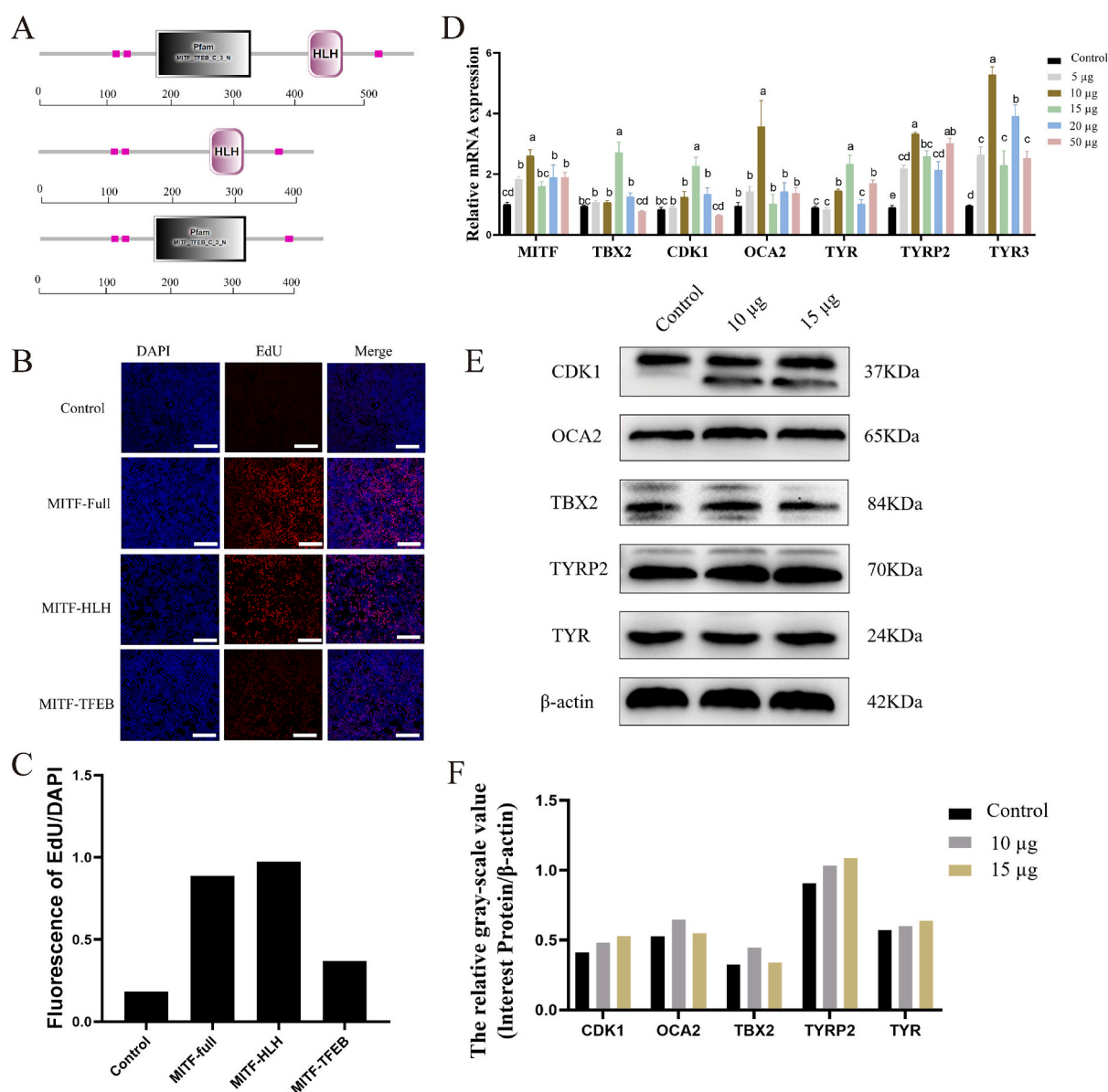


**Fig. 3.** MITF overexpression enhances cell proliferation and upregulates melanogenesis-related gene expression. (A) Domain structure of the full-length MITF, the truncated mutant lacking the TFEB domain, and the truncated mutant lacking the bHLH domain. (B) Edu assays to confirm that different domain of MITF overexpression promotes cell proliferation. HEK293T cells were transfected with empty plasmid, full-length MITF and truncated MITF. Edu (red) was utilized to detect the proliferating cells by labeling the newly synthesized DNA, while DAPI (blue) was used to measure the background by staining total cellular DNA. (scale bar = 250 μm). (C) The images were digitalized using Image J to quantify the fluorescence signals from EdU and DAPI fluorescence signals. (D) The recombinant protein of MITF incubated with black mantle tissues in vitro. qRT-PCR quantification of pigmentation genes and melanocyte proliferation genes. (E) Western blot analysis of CDK1, OCA2, TBX2, TYRP2, TYR, and normalization by β-actin, on treatment with MITF protein. (F) The relative protein expression was analyzed and represented by a histogram. Data were presented as means ± SD ( $n = 3$ ). The significant difference ( $P < 0.05$ ) was indicated by different lowercase letters.

assessed tyrosinase activity and melanin content, confirming a significant reduction in both (Fig. 4-C, D). Furthermore, electron microscopic evaluation of ML329 injection confirmed that the melanosomes in the melanocytes exhibited pigmentation uneven, while the control group displayed relatively dense melanosome pigmentation (Fig. 4-G). The immunofluorescence of cell proliferation genes like TBX2 and CDK1 exhibited significant decrease. The localization was where melanin pigmentation occurs, indicating that melanocyte proliferation suffered suppression (Fig. 4-H). The immunofluorescence of melanogenesis genes like TYR, and TYRP2 displayed significant suppression, exhibiting a notable reduction in melanogenesis (Fig. 4-H), which were consistent with mRNA and protein expression analysis. The results showed that melanogenesis and melanocyte proliferation were significantly hindered compared to the control group.

### 3.6. MITF directly binds to TBX2 promoter and regulates its expression

To further investigate the induction of TBX2 by MITF, we cloned 2-kb upstream region of TBX2 into a reporter vector and conducted dual-luciferase assays. Luciferase assays confirmed that MITF could enhance luciferase activity (Fig. 5-A). Additionally, different domains were found to induce luciferase activity. Specifically, the bHLH domain exhibited a significant increase in luciferase activity compared to both the full-length MITF and the TFEB domain of MITF (Fig. 5-A). The analysis of E-box motifs in the TBX2 promoter regions and their detection through mutated assays were performed using dual-luciferase assays. The results revealed that co-transfected with the bHLH domain of MITF exhibited the reduction of luciferase activity with binding sites mutation (Fig. 5-B). Furthermore, we observed that two binding sites contribute to MITF

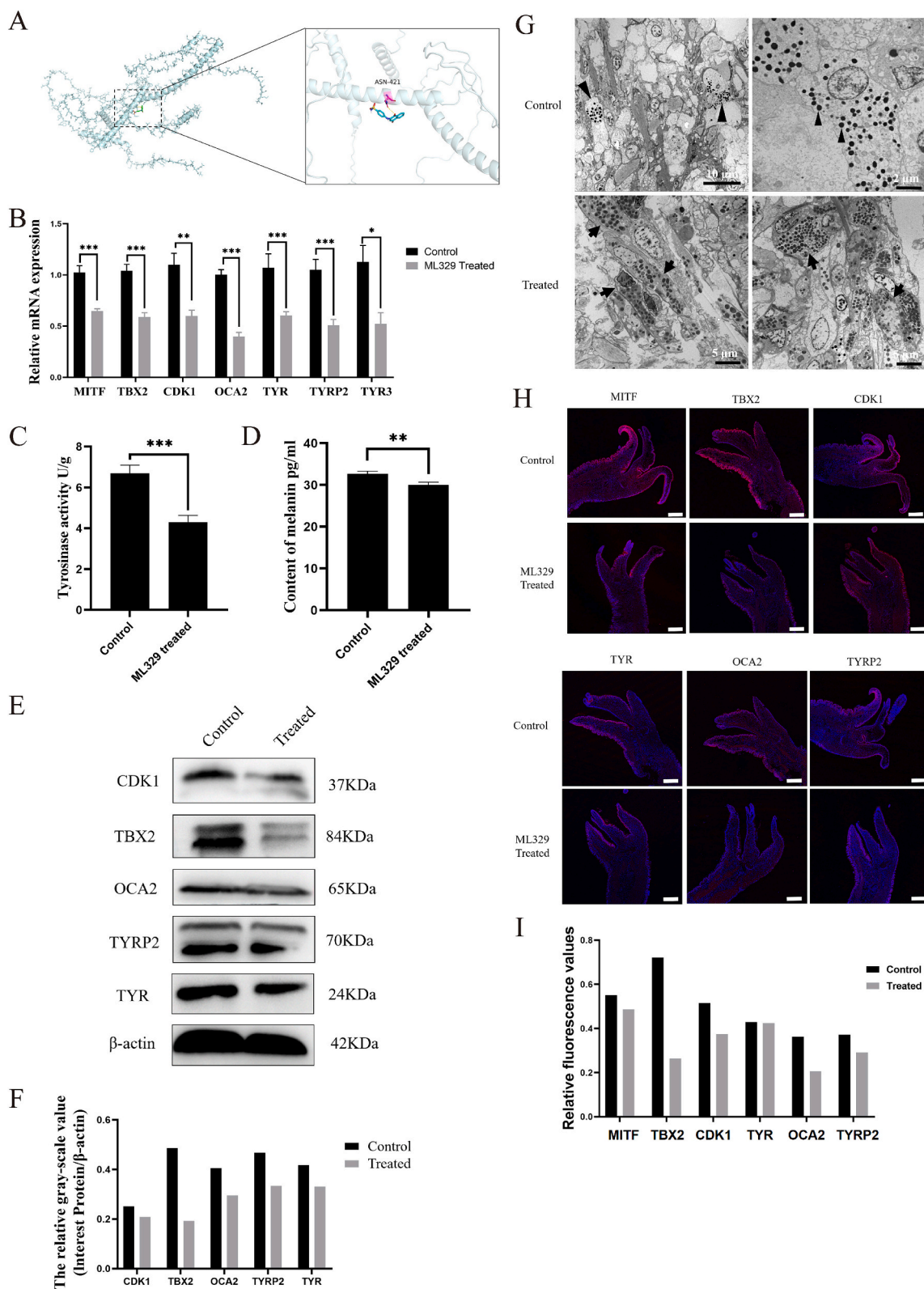


**Fig. 4.** In vivo MITF inhibitor injection reduces melanocytes proliferation and melanin synthesis. (A) Molecular docking using Autodock predicted an interaction between the MITF small-molecule inhibitor ML329 and CgMITF. (B) The RNA level of MITF, TBX2, CDK1, OCA2, TYRP2, TYR3, TYR4 were detected after injected with ML329. (C)(D) The tyrosinase activity and the content of melanin were detected after ML329 injection. (E) Western blot analysis of CDK1, OCA2, TBX2, TYRP2, TYR, and normalization by β-actin, on treatment with ML329 inhibitor. (F) Protein band density was calculated using Image J software. (G) After *C. gigas* was injected with MITF inhibitor, TEM analysis revealed melanogenesis defect. The black triangle in the control group represented normal melanosome, while the black arrows in the treated group displayed melanogenesis defect in the melanocyte, pigment deposition uneven. (H) The immunofluorescence of MITF, TBX2, CDK1, TYR, TYRP2, and OCA2 after treated with ML329. (scale bar = 250 μm). (I) Data were presented as means ± SD (n = 3). Asterisks indicate significant differences between groups: \*  $p < 0.05$ , \*\*  $p < 0.01$ , \*\*\*  $p < 0.001$  by one-way ANOVA.

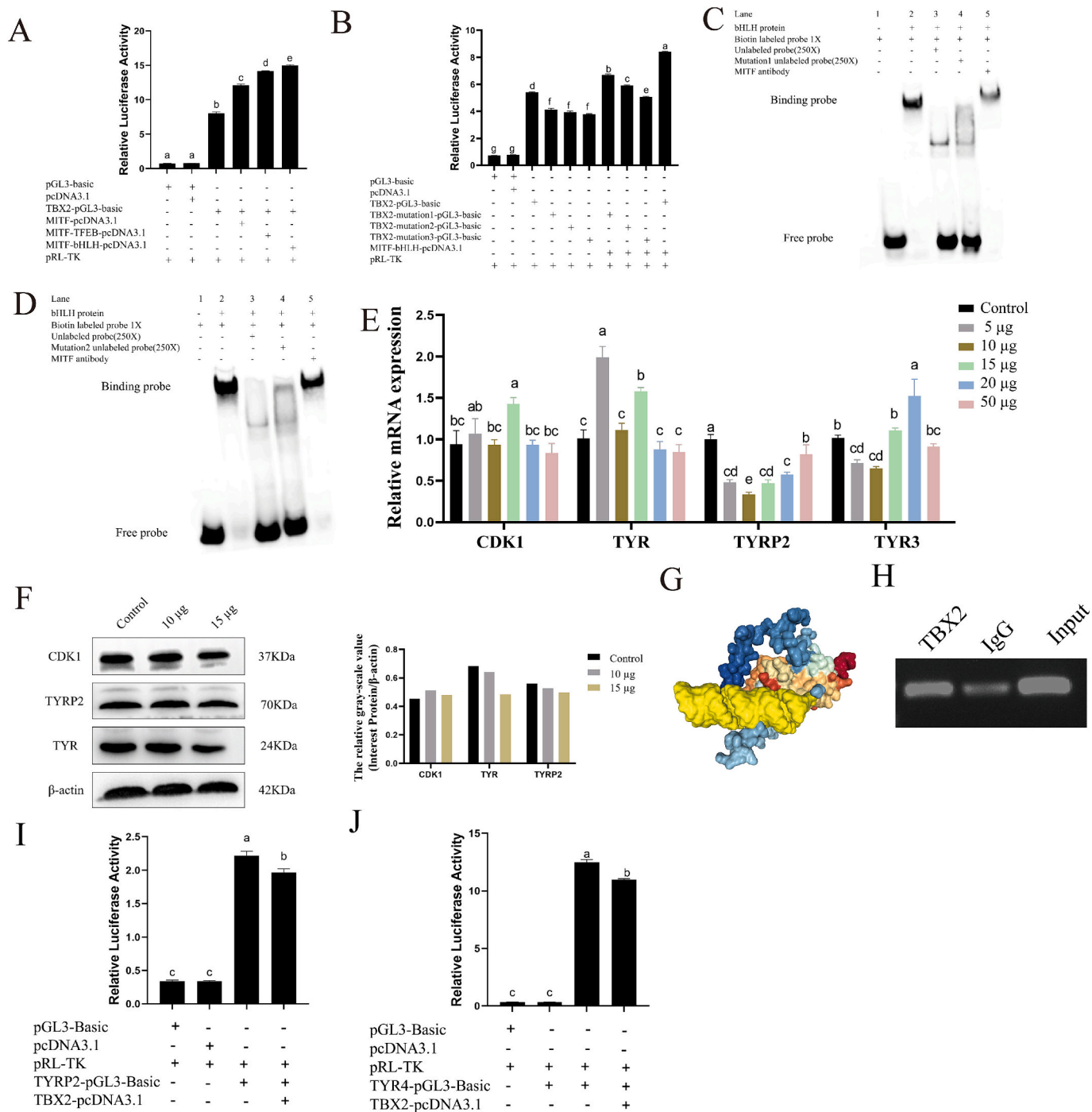


**Fig. 5.** Regulatory interaction involving MITF, TBX2, and CDK1 in melanocyte cell cycle control. (A) Effect of different domain of MITF on the activity of TBX2 promoter in HEK293T cells. (B) Effect of site mutation of TBX2 promoter region detected by the dual-luciferase reporter activity assay. (C) (D) Binding of MITF to the response region as determined by EMSA. (E) The mRNA expression detection on the treatment with the TBX2 protein incubation. (F) The relative protein quantification was analyzed by western blot. (G) Protein band density was calculated using Image J software. (H) Molecular docking using HDock server predicted that TBX2 promoter region interaction with CDK1 protein. (I) TBX2 directly binds with the specific promoter region of the CDK1 as determined by the ChIP-PCR experiments. (J)(K) TBX2 inhibits the transcriptional activity of the TYR promoter via the dual-luciferase activity assays. Data were presented as means ± SD (n = 3). The significant difference ( $P < 0.05$ ) was indicated by different lowercase letters.

responsiveness, and additionally, the mutation of E-box motifs in the TBX2 promoter can be significantly inhibited (Fig. 5-B). Direct binding was evaluated using two E-box motifs as a probe in EMSA. The shift was abrogated with an E-box cold-competitor probe and mutated probe (Fig. 5-C, D). Thus, we established that the melanocyte proliferation pathway controls TBX2 expression via direct binding of MITF to the TBX2 promoter, which mediates downstream effector genes.

Given that TBX2 was a MITF downstream effector gene, and considering its relationship with tyrosinase-related genes and cyclin D1 gene in influencing the cell cycle, we then conducted to incubate TBX2 protein with black mantle tissues in vitro. mRNA expression of CDK1 significantly increased at a dosage of 15 µg, while at other dosages, there was no significant change (Fig. 5-E). The protein expression of CDK1 increased at the dosages of 10 µg and 15 µg (Fig. 5-F). Additionally,

HDock online software predicted an interaction with the CDK1 promoter region and TBX2 (Fig. 5-G). Chromatin immunoprecipitation using TBX2 polyclonal antibody to TBX2 demonstrated that TBX2 could directly bind to the promoter of CDK1 in *C. gigas* (Fig. 5-H). Melanogenesis-related genes exhibited inhibition both in mRNA expression level and protein expression level in general (Fig. 5-E, F). The dual-luciferase activity was inhibited when co-transfected with the TYR related genes promoter and TBX2 transcription factor (Fig. 5-I, J), consistent with the protein levels. These results suggested that TBX2 has dual functions, including transcription activation and transcription inhibition.

## 4. Discussion

### 4.1. Molecular modularity of mantle tissues

The diversity in morphology can be attributed to the influence of genes governing development, with various genetic mechanisms potentially contributing to variability in gene activity [20]. Bivalve shell color is primarily determined by the mantle tissues [21–23]. The mantle tissues are segmented into three zones based on their specific functions: the outer fold for secretion, the inner fold for muscular movement, and the middle fold for sensory perception [24]. The tissue's functional module is associated with genes/proteins that coordinate to execute specific functions [25]. We characterized the expression patterns of five genes related to melanogenesis and melanocyte proliferation. These genes were distributed across three folds, but were not completely synchronized with the melanin distribution pattern. It is likely that these genes not only participate in melanogenesis but also in melanin secretion. The deposition of melanin in the inner fold and middle fold suggested that melanin originate from these regions. Additionally, the distribution of acetylation aligned with melanin deposition, suggesting that the inner and middle fold regions exhibited higher activity in gene transcription and protein synthesis associated with melanogenesis mediated by acetylation. These two zones were likely to possess proteins specifically modified, such as acetylation, for functionality. We hypothesized that acetylation distribution modules in the mantle tissues were associated with gene regulatory networks that specify zones within the mantle tissues for melanogenesis.

### 4.2. p300-mediated acetylation leads to MITF transcriptional activity

The transcriptional activity of MITF is regulated by various mechanisms, involving a diverse set of post-translational modifications, which are crucial for regulating protein stability, activity, subcellular localization, and binding with co-factors [26]. Specially, lysine acetylation is well known to regulate protein-protein [27,28], and protein-DNA interactions [29]. Histone acetylation is the most frequently reported histone modification in melanogenesis [30]. Evidence from multiple sources highlighted the crucial role of p300/CBP in MITF-mediated gene expression in melanogenesis. Functionally, p300, with its histone acetyltransferase (HAT) function, catalyzed acetylation on the core domains of histones, while also facilitating lysine acetylation of various proteins [31]. Our study confirmed that p300 function as co-activator, not only enhancing MITF promoter activity but also facilitating the binding of the MITF transcription factor to the tyrosinase promoter. Previous research has also underscored the pivotal role of p300 in melanosomal pH regulation mediated by CA14, as it actively facilitated H3K27 acetylation, ultimately driving gene activation [9]. Our study revealed that inhibition of p300 activity significantly reduced downstream gene expression, and diminished the binding affinity of MITF-targeted proteins. This has confirmed that the protein stability of MITF and the functioning of its downstream genes can be regulated by upstream p300-mediated acetylation. It has been reported that the protein stability of MITF was tightly regulated by ubiquitination and subsequent proteasomal degradation [32,33]. Therefore, the interplay

between acetylation and ubiquitination, lysine modification, impacted the stability and activity of MITF and its downstream protein.

Furthermore, the bHLH domain of CgMITF was predicted to contain crucial lysine residues for MITF functionality. Notably, K6, among the predicted acetylation sites, exhibits high conservation and was essential for binding with the E-box motif of melanogenesis-related genes in *C. gigas*, identical to the K206 in humans. Previous research has shown that p300/CBP-mediated acetylation of K206 inhibits MITF's DNA binding ability, leading to decreased affinity [34]. Experimental evidence showed that K206Q mutant (acetylation mimetic) failed to efficiently complement the absence of MITF, indicating defective gene expression [34]. Furthermore, it has been observed that the acetylation of K206 can decrease the genome-wide MITF DNA-binding affinity, favoring binding away from differentiation-associated motifs [34], suggesting a suppression of differentiation. However, the impact of K206 acetylation on melanocyte development may vary depending on the developmental stages, potentially involving processes of both acetylation and deacetylation. Therefore, residues like K6 in the Pacific oyster, equivalent to K206 in humans, likely undergo dynamic acetylation modulation depending on the stages of melanocyte development. This modulation led to a redistribution of binding-motif bias across the genome, thereby regulating the availability of transcription factor and modulating DNA affinity to trigger different functions.

Another crucial lysine residue for MITF functionality in the *C. gigas* was K43, equivalent to K243 in humans, was highly conserved in most bHLH transcription factors and contacted the phosphate backbone in the available E-box motif crystal structure. Significantly, prior research has shown that the status of MITF K243 was a key determinant of melanocyte development [6]. The acetylation mimetic K243Q mutant demonstrated reduced DNA-binding affinity in vitro but supports melanocyte development more effectively than the non-acetylatable K243R mutant with higher affinity [6]. This close correspondence between K6 (in *C. gigas*) and K206 (in human), as well as K43 (in *C. gigas*) and K243 (in human) highlighted the significance of its regulatory mechanism across species. This demonstrated that potential acetylated lysine residues undergo redistribution of binding-motif bias and functionally regulate MITF's access to DNA with different functions.

### 4.3. MITF's dynamic leucine zipper interacts with E-box motif, determining melanocyte fate

MITF is a master regulator in the development of melanocyte. The predicted structure of MITF is largely disordered, with the exception of a conserved bHLH-LZ domain. This domain facilitated MITF dimerization. Additionally, the basic region forms a helical structure and directly interacted with the E box or M box DNA sequence found on the promoters of MITF target genes [35,36]. In our experiment, the mutation of K6 and K43 within bHLH domain evidently reduced the affinity of the E-box motif for the tyrosinase promoter, therefore we confirmed that mutations in the bHLH region resulted in damage to the function of MITF. Moreover, the MITF small-molecule inhibitor ML329 was administered to the *C. gigas*. Molecular docking analysis demonstrated that ML329 has the potential to interact with the specific amino acid within the bHLH domain, possibly leading to the disruption of MITF dimerization and its functional activity. Functional assays revealed that treatment with this inhibitor significantly weakened the expression of downstream genes and hindered melanogenesis. Previous research has shown that mutations or small-molecule compounds can weaken the dimer, causing a shift in equilibrium towards the non-structured monomeric form [37]. This trapped MITF in a lower energy state, establishing an energy barrier that effectively obstructs MITF from refolding [37]. Consequently, the failure of bHLH domain dimerization completely hampers its ability to bind to DNA and carry out transcription activities.

The bHLH domain of MITF not only recognizes DNA motifs known as E-boxes, but has also serves various functions, including the regulation

of cell proliferation, and the influence on the development of specific cell lineages [38]. In *Arabidopsis thaliana*, the formation of bHLH transcription factor heterodimers acted as the general regulator of cell proliferation in meristems [39]. Additionally, previous research has reported that the insertion of six residues located upstream of the DNA binding basic domain strongly inhibits DNA synthesis [38], suggesting that changes in the bHLH domain can affect cell proliferation. Our experiments also confirmed that the bHLH domain played an invaluable role in cell proliferation, as verified in the 293 T cells. The results demonstrated that the bHLH domain of MITF served as a link in the regulation of cell proliferation genes.

#### 4.4. MITF-TBX2 axis collaborates with CDK1 to regulate melanocyte development

Here we reported that TBX2 is one of MITF known targeted genes in melanocyte proliferation regulation. Many studies have reported that cis-elements, such as E-box, which is essential for the transcriptional activation of melanogenesis-related genes by recruiting the transcription factors, including MITF [40]. In our study, site-directed mutagenesis significantly reduced the binding activity between the E-box motif in the TBX2 promoter region and MITF. Similarly, a recent study has demonstrated that the E-box variant impaired the transcription ability of TYR promoter by impeding MITF binding [41]. Other study found that upstream transcription factor 11 failed to bind the E-box variant on the promoter of splicing gene ESRP1 [42]. This further underscored the specificity of E-box motifs within distinct gene regulatory context.

Previous studies have shown that TBX2 participated in cell cycle regulation and malignant transformation [43]. Our study confirmed that TBX2 regulates melanocyte proliferation by stimulating expression of CDK1, which was conserved in human melanocyte proliferation. Interestingly, research has also reported that TBX2 controls melanogenesis by repressing OCA2 [44], which was in line with our results showing that TYR related genes were repressed by TBX2. The findings suggested that TBX2 possesses dual functionality, including transcription activation and transcription inhibition. It is plausible that TBX2's activity may be influenced by unknown feedback loops within cellular regulatory network, which may account for its dual functionality.

## 5. Conclusion

In summary, we have demonstrated that acetylation pattern is closely related to melanogenesis process. Specially, several of the MITF target genes (like TYR, TBX2) exhibit direct activation mediated by E-box elements binding with the bHLH domain of MITF, regulating melanogenesis and cell proliferation. Additionally, the recruitment of co-activator p300 facilitated MITF dynamic interaction to downstream targeted gene promoters. Taken together, our findings revealed how post-translational modification of MITF modulated its targeting binding, influencing gene expression programs vital of melanocyte proliferation and differentiation in *C. gigas*.

Supplementary data to this article can be found online at <https://doi.org/10.1016/j.ijbiomac.2024.131138>.

## CRediT authorship contribution statement

**Yue Min:** Writing – original draft, Visualization, Validation, Investigation. **Hong Yu:** Methodology, Formal analysis. **Qi Li:** Writing – review & editing, Supervision, Resources, Project administration, Funding acquisition, Conceptualization.

## Declaration of competing interest

The authors declare that they have no known competing financial interests or personal relationships that could have appeared to influence the work reported in this paper.

## Data availability

No data was used for the research described in the article.

## Acknowledgements

This work was supported by grants from National Natural Science Foundation of China (32373115), Shandong Province (2022LZGCQY010, 2021ZLGX03 and 2021LZGC027), and Agriculture Research System of China Project (CARS-49).

## References

- [1] T. Hirobe, How are proliferation and differentiation of melanocytes regulated? *Pigment Cell Melanoma Res.* 24 (3) (2011) 462–478.
- [2] R. Gupta, R. Janostiak, N. Wajapeyee, Transcriptional regulators and alterations that drive melanoma initiation and progression, *Oncogene* 39 (48) (2020) 7093–7105.
- [3] S.A. D'Mello, G.J. Finlay, B.C. Baguley, M.E. Askarian-Amiri, Signaling pathways in melanogenesis, *Int. J. Mol. Sci.* 17 (7) (2016) 1144.
- [4] A. Kawakami, D.E. Fisher, The master role of microphthalmia-associated transcription factor in melanocyte and melanoma biology, *Lab. Invest.* 97 (6) (2017) 649–656.
- [5] M. Hejna, W.M. Moon, J. Cheng, A. Kawakami, D.E. Fisher, J.S. Song, Local genomic features predict the distinct and overlapping binding patterns of the bHLH-zip family oncoproteins MITF and MYC-MAX, *Pigment Cell Melanoma Res.* 32 (4) (2019) 500–509.
- [6] P. Lophrasitthiphol, R. Siddaway, A. Loffreda, V. Pogenberg, F. Friedrichsen, D. Sheinboim, I. Dror, L. Thomas, C. Cossou, P. Gonen, Y. Stanevsky, R. Brenner, T. Perluk, J. Frand, S. Elgavish, Y. Nevo, D. Rahat, Y. Tabach, M. Khaled, S.S. Shen-Orr, C. Levy, UV-protection timer controls linkage between stress and pigmentation skin protection systems, *Mol. Cell* 72 (3) (2018) 444–456.
- [7] D.A. Raja, V. Gotherwal, S.A. Burse, Y.J. Subramaniam, F. Sultan, A. Vats, H. Gautam, B. Sharma, S. Sharma, A. Singh, S. Sivasubbu, R.S. Gokhale, V. T. Natarajan, pH-controlled histone acetylation amplifies melanocyte differentiation downstream of MITF, *EMBO Rep.* 21 (1) (2020) e48333.
- [8] R. Dilshat, H.N. Vu, E. Steingrimsdottir, Epigenetic regulation during melanocyte development and homeostasis, *Exp. Dermatol.* 30 (8) (2021) 1033–1050.
- [9] V.E. Papaioannou, The T-box gene family: emerging roles in development, stem cells and cancer, *Development* 141 (20) (2014) 3819–3833.
- [10] B. Bilican, C.R. Goding, Cell cycle regulation of the T-box transcription factor TBX2, *Exp. Cell Res.* 312 (12) (2006) 2358–2366.
- [11] S. Carreira, B. Liu, C.R. Goding, The gene encoding the T-box factor Tbx2 is a target for the microphthalmia-associated transcription factor in melanocytes, *J. Biol. Chem.* 275 (29) (2000) 21920–21927.
- [12] F. Liu, J. Cao, J. Lv, L. Dong, E. Pier, G.X. Xu, R.A. Wang, Z. Xu, C. Goding, R. Cui, TBX2 expression is regulated by PAX3 in the melanocyte lineage, *Pigment Cell Melanoma Res.* 26 (1) (2013) 67–77.
- [13] K.W. Vance, S. Carreira, G. Brosh, C.R. Goding, TBX2 is overexpressed and plays an important role in maintaining proliferation and suppression of senescence in melanomas, *Cancer Res.* 65 (6) (2005) 2260–2268.
- [14] L. Pan, X. Ma, B. Wen, Z. Su, X. Zheng, Y. Liu, H. Li, Y. Chen, J. Wang, F. Lu, J. Qu, L. Hou, Microphthalmia-associated transcription factor/T-box factor-2 axis acts through cyclin D1 to regulate melanocyte proliferation, *Cell Prolif.* 48 (6) (2015) 631–642.
- [15] S. Carreira, T.J. Dexter, U. Yavuzer, D.J. Easty, C.R. Goding, Brachyury-related transcription factor TBX2 and repression of the melanocyte-specific TRP-1 promoter, *Mol. Cell. Biol.* 18 (9) (1998) 5099–5108.
- [16] C.A. Schneider, W.S. Rasband, K.W. Eliceiri, NIH image to ImageJ: 25 years of image analysis, *Nat. Methods* 9 (7) (2012) 671–675.
- [17] Y. Cheli, M. Ohanna, R. Ballotti, C. Bertolotto, Fifteen-year quest for microphthalmia-associated transcription factor target genes, *Pigment Cell Melanoma Res.* 23 (1) (2010) 27–40.
- [18] P. Simpson, The stars and stripes of animal bodies: evolution of regulatory elements mediating pigment and bristle patterns in *Drosophila*, *Trends Genet.* 23 (7) (2007) 350–358.
- [19] Y.J. Zhu, Q. Li, H. Yu, S.K. Liu, Pigment distribution and secretion in the mantle of the Pacific oyster (*Crassostrea gigas*), *J. Ocean Univ. China* 22 (2023) 813–820.
- [20] J.H. Kang, H.S. Kang, J.M. Lee, C.M. An, S.Y. Kim, Y.M. Lee, J.J. Kim, Characterizations of shell and mantle edge pigmentation of a Pacific oyster, *Crassostrea gigas*, in Korean peninsula, *Asian Australas. J. Anim. Sci.* 26 (12) (2013) 1659–1664.

- [23] J. Mao, W. Zhang, X. Wang, J. Song, D. Yin, Y. Tian, Z. Hao, B. Han, Y. Chang, Histological and expression differences among different mantle regions of the yesso scallop (*Patinopecten yessoensis*) provide insights into the molecular mechanisms of biomineralization and pigmentation, *Mar. Biotechnol.* (N.Y.) 21 (5) (2019) 683–696.
- [24] J.A. Audino, J.E. Marian, A. Wanninger, S.G. Lopes, Mantle margin morphogenesis in *Nodipecten nodosus* (Mollusca: Bivalvia): new insights into the development and the roles of bivalve pallial folds, *BMC Dev. Biol.* 15 (2015) 22.
- [25] G.P. Wagner, M. Pavlicev, J.M. Cheverud, The road to modularity, *Nat. Rev. Genet.* 8 (12) (2007) 921–931.
- [26] J.M. Lee, H.M. Hammarén, M.M. Savitski, S.H. Baek, Control of protein stability by post-translational modifications, *Nat. Commun.* 14 (1) (2023) 201.
- [27] L.M. Myklebust, P. Van Damme, S.I. Støve, M.J. Dörfel, A. Abboud, T.V. Kalvik, C. Grauffel, V. Jonckheere, Y. Wu, J. Swensen, H. Kaasa, G. Liszczak, R. Marmorstein, N. Reuter, G.J. Lyon, K. Gevaert, T. Arnesen, Biochemical and cellular analysis of Ogden syndrome reveals downstream nt-acetylation defects, *Hum. Mol. Genet.* 24 (2015) 1956–1976.
- [28] E. Linster, F.L. Forero Ruiz, P. Miklankova, T. Ruppert, J. Mueller, L. Armbruster, X. Gong, G. Serino, M. Mann, R. Hell, M. Wirtz, Cotranslational n-degron masking by acetylation promotes proteome stability in plants, *Nat. Commun.* 13 (1) (2022) 810.
- [29] A. Mayer, N.R. Siegel, A.L. Schwartz, A. Ciechanover, Degradation of proteins with acetylated amino termini by the ubiquitin system, *Science* 244 (1989) 1480–1483.
- [30] S. Zhou, H. Zeng, J. Huang, L. Lei, X. Tong, S. Li, Y. Zhou, H. Guo, M. Khan, L. Luo, R. Xiao, J. Chen, Q. Zeng, Epigenetic regulation of melanogenesis, *Ageing Res. Rev.* 69 (2021) 101349.
- [31] B.M. Dancy, P.A. Cole, Protein lysine acetylation by p300/CBP, *Chem. Rev.* 115 (6) (2015) 2419–2452.
- [32] S. Hu, S. Bai, Y. Dai, N. Yang, J. Li, X. Zhang, F. Wang, B. Zhao, G. Bao, Y. Chen, X. Wu, Deubiquitination of MITF-M regulates melanocytes proliferation and apoptosis, *Front. Mol. Biosci.* 8 (2021) 692724.
- [33] X.S. Zhao, B. Fiske, A. Kawakami, J.Y. Li, D.E. Fisher, Regulation of MITF stability by the USP13 deubiquitinase, *Nat. Commun.* 2 (2011) 414.
- [34] P. Louphrasitthiphol, A. Loffreda, V. Pogenberg, S. Picaud, A. Schepsky, H. Friedrichsen, Z. Zeng, A. Lashgari, B. Thomas, E.E. Patton, M. Wilmanns, P. Filippakopoulos, J.P. Lambert, E. Steingrímsson, D. Mazza, C.R. Goding, Acetylation reprograms MITF target selectivity and residence time, *Nat. Commun.* 14 (1) (2023) 6051.
- [35] T.J. Hemesath, E. Steingrímsson, G. McGill, M.J. Hansen, J. Vaught, C. A. Hodgkinson, H. Arnheiter, N.G. Copeland, N.A. Jenkins, D.E. Fisher, Microphthalmia, a critical factor in melanocyte development, defines a discrete transcription factor family, *Genes Dev.* 8 (22) (1994) 2770–2780.
- [36] V. Pogenberg, M.H. Ogmundsdóttir, K. Bergsteinsdóttir, A. Schepsky, B. Phung, V. Deineko, M. Milewski, E. Steingrímsson, M. Wilmanns, Restricted leucine zipper dimerization and specificity of DNA recognition of the melanocyte master regulator MITF, *Genes Dev.* 26 (23) (2012) 2647–2658.
- [37] Z. Liu, K. Chen, J. Dai, P. Xu, W. Sun, W. Liu, Z. Zhao, S.P. Bennett, P. Li, T. Ma, Y. Lin, A. Kawakami, J. Yu, F. Wang, C. Wang, M. Li, P. Chase, P. Hodder, T. P. Spicer, L. Scampavia, C. Cao, L. Pan, J. Dong, Y. Chen, B. Yu, M. Guo, P. Fang, D. E. Fisher, J. Wang, A unique hyperdynamic dimer interface permits small molecule perturbation of the melanoma oncoprotein MITF for melanoma therapy, *Cell Res.* 33 (1) (2023) 55–70.
- [38] K. Bismuth, D. Maric, H. Arnheiter, MITF and cell proliferation: the role of alternative splice forms, *Pigment Cell Res.* 18 (5) (2005) 349–359.
- [39] E. Mor, M. Pernisová, M. Minne, G. Cerutti, D. Ripper, J. Nolf, J. Andres, L. Ragni, M.D. Zurbriggen, B. De Rybel, T. Vernoux, bHLH heterodimer complex variations regulate cell proliferation activity in the meristems of *Arabidopsis thaliana*, *iScience* 25 (11) (2022) 105364.
- [40] J.M. Um, H.J. Kim, Y. Lee, C.H. Choi, D. Hoang Nguyen, H.B. Lee, J.H. Shin, K. Tai No, E.K. Kim, A small molecule inhibitor of Mitf-E-box DNA binding and its depigmenting effect in melan-a cells, *J. Eur. Acad. Dermatol. Venereol.* 26 (10) (2012) 1291–1297.
- [41] C. Li, Q. Chen, J. Wu, J. Ren, M. Zhang, H. Wang, J. Li, Y. Tang, Identification and characterization of two novel noncoding tyrosinase (TYR) gene variants leading to oculocutaneous albinism type 1, *J. Biol. Chem.* 298 (5) (2022) 101922.
- [42] K. Zeng, B. He, B.B. Yang, T. Xu, X. Chen, M. Xu, X. Liu, H. Sun, Y. Pan, S. Wang, The pro-metastasis effect of circANKS1B in breast cancer, *Mol. Cancer* 17 (1) (2018) 160.
- [43] A. Abrahams, M.I. Parker, S. Prince, The T-box transcription factor TBX2: its role in development and possible implication in cancer, *IUBMB Life* 62 (2) (2010) 92–102.
- [44] Y. Chen, L. Pan, Z. Su, J. Wang, H. Li, X. Ma, Y. Liu, F. Lu, J. Qu, L. Hou, The transcription factor TBX2 regulates melanogenesis in melanocytes by repressing OCA2, *Mol. Cell. Biochem.* 415 (1–2) (2016) 103–109.